Hepatocytes from α_{1B}-adrenoceptor knockout mice reveal compensatory adrenoceptor subtype substitution

*,[1]Clare Deighan, [1]Alison M. Woollhead, [1]Janet F. Colston & [1]John C. McGrath

[1]Autonomic Physiology Unit, Division of Neuroscience and Biomedical Systems, Institute of Biomedical and Life Sciences, University of Glasgow, Glasgow, G12-8QQ

1 α_1-Adrenoceptors (ARs) play an important functional role in the liver; yet little is known about their cellular location. We identified the subtypes present in wild-type (WT) and α_{1B}-AR knockout (KO) mice livers at 3 and 4 months of age, and investigated their distribution in hepatocytes.

2 The fluorescent α_1-AR antagonist quinazolinyl piperazine borate-dipyrromethene (QAPB) was used to visualise hepatic α_1-ARs and radioligand binding with [^{3}H]-prazosin was used to quantify the α_1-AR population.

3 QAPB and [^{3}H]-prazosin bound specifically to hepatic α_1-ARs with nanomolar affinity. The cellular distribution of α_1-ARs was similar in WT and α_{1B}-AR KO hepatocytes; QAPB binding was distributed diffusely throughout the cell with no binding evident on the plasma membrane. Radioligand binding produced B_{max} values as follows: 3-month WT – 76 ± 3.3 fmol mg^{-1}; 4-month WT – 50 ± 3.1 fmol mg^{-1}; 3-month α_{1B}-AR KO – 7.4 ± 0.73 fmol mg^{-1}; 4-month α_{1B}-AR KO – 30 ± 2.0 fmol mg^{-1}.

4 In 3- and 4-month WT liver, all antagonists acted competitively. RS100329 (α_{1A}-selective) and BMY7378 (α_{1D}-selective) bound with low affinities, indicating the presence of α_{1B}-ARs. In 4-month α_{1B}-AR KO liver prazosin produced a biphasic curve, whereas RS100329 and BMY7378 produced monophasic curves of high and low affinity, respectively, indicating the presence of α_{1A}-ARs.

5 In conclusion, we have made the novel observation that α_1-ARs can compensate for one another in the absence of the endogenously expressed receptor; yet there appears to be no subtype-specific subcellular location of α_1-ARs; the WT livers express α_{1B}-ARs, while α_{1B}-AR KO livers express α_{1A}-ARs. This study provides new insights into both hepatocyte and α_1-AR biology.
British Journal of Pharmacology (2004) **142**, 1031–1037. doi:10.1038/sj.bjp.0705872

Keywords: Confocal laser-scanning microscopy; QAPB; radioligand binding; hepatocyte and adrenergic

Abbreviations: AR, adrenoceptor; GPCR, G-protein-coupled receptor; KO, knockout; QAPB, quinazolinyl piperazine borate-dipyrromethene; WT, wild type

Introduction

Hepatocytes express adrenoceptors (ARs) that modulate several aspects of metabolism, including glycogenolysis, gluconeogenesis, synthesis of urea and fatty acid metabolism (Hieble *et al.*, 1995). Adrenergic hepatic function is mainly under the control of α_1-ARs except in the foetus and neonate, where it has been shown that β-ARs are predominantly expressed (Rossby & Cornett, 1991). Until now, this has been considered to be the only major ontogenic variation in hepatic ARs.

There are three subtypes of α_1-ARs which have been defined by molecular and pharmacological techniques, $\alpha_{1a/A}$, $\alpha_{1b/B}$ and $\alpha_{1d/D}$ (Bylund *et al.*, 1994; Hieble *et al.*, 1995).

In a series of papers, Garcia-Sainz *et al.* (1992; 1995a, b; 1996a) demonstrated that in the liver one α_1-AR subtype dominated in each species but the dominant subtype varied with species. Humans, cat, dog and rabbit expressed the α_{1A}-AR, yet the rat, mouse and hamster expressed the α_{1B}-AR (Garcia-Sainz *et al.*, 1994). The one exception was monkeys, which expressed both α_{1A}-AR and α_{1B}-AR (Garcia-Sainz *et al.*, 1996b).

It is intriguing that different receptor subtypes, which are so well conserved in evolution yet substantially different in structure and location, should apparently serve the same function in the liver of different species. It is possible that subtypes are exchangeable and that external influences upon the organism determine which subtype is dominant in each species.

We have made, and followed up, an observation in mouse that supports this concept. Although the wild-type (WT) mouse expresses only α_{1B}-ARs in its liver (Garcia-Sainz *et al.*, 1994; Cavalli *et al.*, 1997; Yang *et al.*, 1998; Deighan *et al.*, 1999; Deighan & McGrath, 2002), we found that α_{1B}-AR knockout (KO) mouse liver expressed α_{1A}-AR-binding sites between 3 and 4 months (Deighan & McGrath, 2002).

Recent progress in receptor biology has shown that the properties of α_1-AR subtypes, particularly cellular location, can vary dramatically. There is evidence from both recombinant and native receptors in nonhepatic tissues that α_{1A}-ARs have a greater tendency than α_{1B}-ARs to be located intracellularly, rather than be confined to the plasma membrane (Tsujimoto *et al.*, 1998; Hrometz *et al.*, 1999; McGrath *et al.*, 1999; Chalathorn *et al.*, 2002; Sugawara *et al.*,

*Author for correspondence; E-mail: c.deighan@bio.gla.ac.uk

2002). However, as is the case with most attempts to characterise the properties of α_1-AR subtypes, exceptions to the rule are never far away and it now seems that the cellular location of α_1-AR subtypes differs depending on the cell type studied (Stanasila *et al.*, 2003; Hague *et al.*, 2004).

We investigated whether there is a shift in the location of α_1-ARs in hepatocytes when the α_{1A}-AR replaces the α_{1B}-AR in the α_{1B}-AR KO mouse using fluorescent receptor binding. This technique allows analysis of receptor distribution and binding characteristics at the cellular and subcellular levels (Daly *et al.*, 1998; McGrath *et al.*, 1999; Mackenzie *et al.*, 2000), employing the fluorescent α_1-AR antagonist quinazolinyl piperazine borate-dipyrromethene (QAPB) (Daly *et al.*, 1998). Our results were unexpected. There was no detectable difference in the cellular location and distribution of α_{1A}- or α_{1B}-ARs. In contrast to all other tissue types studied, where receptors were found in distinct clusters as well as diffusely throughout the cell (Daly *et al.*, 1998; McGrath *et al.*, 1999; Mackenzie *et al.*, 2000), the receptors in mouse hepatocytes were distributed homogeneously throughout the cytoplasm. Distribution between groups of cells in the liver was, however, heterogeneous; some cells expressed α_1-ARs while other cells did not. This unusual intracellular and intercellular distribution may indicate a general phenomenon in the location and distribution of G-protein-coupled receptors (GPCR), or may be unique to the liver.

Methods

Animals

Male C57 Black/129Sv WT and α_{1B}-AR KO mice, 3- and 4-month old (previously described by Cavalli *et al.*, 1997) were obtained from the Central Research Facility at the University of Glasgow. Animals were obtained on a 12 : 12 h light/dark schedule at 22–25°C and *fed ad libitum* on a standard rodent diet and tap water. All mice were killed by cervical dislocation. Livers were removed and washed in ice-cold Tris–HCl buffer (pH 7.4) before being placed in Hepatocyte Perfusion Media (37°C) for isolation of hepatocytes or being frozen in liquid nitrogen for isolation of membranes.

Hepatocyte isolation and culture

Hepatocytes were isolated by a nonperfusion procedure performed without vascular access by multiple injections into the hepatic parenchyma (adapted from David *et al.*, 1998). The liver portion was placed in a sterile universal containing Hepatocyte Perfusion Media and incubated for ∼1 h at 37°C. This same buffer was then injected using a 10 ml syringe *via* an 18 G needle into all areas of the liver until the tissue softened and a cell suspension was released. The flow rate was approximately 10 ml min^{-1}. The solution was not re-circulated. The cell suspension was centrifuged at 50 × *g* for 1 min at 20°C. The cell pellet was washed twice with Hepatocyte Attachment Media at 50 × *g* for 1 min to isolate hepatocytes from other cell types. Cell viability was determined by Trypan Blue exclusion. The cell pellet was finally resuspended in a minimal volume of Attachment Media and cells were allowed to attach to glass cover slips.

Generation of liver slices

Livers were removed from the animal and sections were cut using a sterile blade. Slices were incubated with 20 nM QAPB for 30 min at 20°C, then mounted on slides in a fluorescent mounting medium (DAKO). A higher concentration of QAPB was required, than was used for heptocytes to allow for penetration of the QAPB through the tissue.

Confocal microscopy

Coverslips were mounted in a flow chamber (WPI) and placed on the stage of an invert (Nikon Diaphot) microscope fitted with a Noran Odyssey Laser-Scanning Confocal Module. The objective used was a Nikon × 40, oil. Images were collected and analysed using Metamorph software. Fluorophores were excited using a 488 nm argon laser and detected with a 515 nm band-pass filter. In all experiments, a 15 μm slit was used and all other parameters were kept constant.

QAPB saturation curves   The system was set to acquire images at 1-min intervals. After a baseline was established, a cumulative concentration–response curve was carried out to QAPB (0.4–20 nM) at 20°C, with 5-min intervals between concentrations to allow for equilibration. Individual cells were outlined using Metamorph's define-region tool and the fluorescent intensity values representative of each concentration at equilibrium were recorded. Nonspecific binding was defined as fluorescent binding in the presence of 1 μM prazosin.

Inhibition of QAPB-associated fluorescence binding   Experiments were carried out in a similar manner to saturation curves, except that hepatocytes were incubated for 30 min with the α_{1A}-AR selective antagonist RS100329 (Williams *et al.*, 1999) (1 nM) or the α_{1D}-AR selective antagonist BMY7378 (Goetz *et al.*, 1995) (1 nM) prior to addition of 5 nM QAPB. The ability of either drug to inhibit the development of QAPB-associated fluorescence has already been demonstrated (Mackenzie *et al.*, 2000). The measure of 1 nM is effective only against the subtype for which each is selective and does not affect the other subtypes. The published K_B/K_i values for RS100329 are: α_{1A}-AR, 0.25 nM; α_{1B}- and α_{1D}-AR, 15 nM (Williams *et al.*, 1999). Therefore, at 1 nM, RS100329 will occupy ∼80% of α_{1A}-AR, while occupying only 6% of α_{1B}- or α_{1D}-ARs. BMY7378 has affinities: α_{1D}-AR, 0.03 nM; α_{1A}-AR, 80 nM; α_{1B}-AR, 160 nM (Mackenzie *et al.*, 2000). Therefore, at a concentration of 1 nM, BMY7378 would occupy more than 95% of α_{1D}-ARs, but less than 2% of α_{1A}- or α_{1B}-ARs.

Membrane isolation

Livers were pulverised under liquid nitrogen, suspended in 50 mM Tris–HCl and homogenised on ice using a pre-cooled polytron at setting 6 for 3–4 × 10–15 s. Liver homogenates were filtered through two layers of muslin and centrifuged at 1200 × *g* for 5 min at 4°C. The supernatant was removed, kept on ice and the pellet was resuspended. This homogenisation/centrifugation step was repeated a total of four times, the supernatants pooled and centrifuged at 56,000 × *g* for 2 × 30 min at 4°C. The resulting pellet was resuspended in 50 mM Tris–HCl and a Pearce protein assay was used to determine the concentration of protein.

Radioligand binding

[³H]prazosin saturation curves Liver membranes (0.5 mg ml⁻¹ of protein) were incubated with a range of [³H]prazosin concentrations (0.025–5 nM, 75 Ci mmol⁻¹) in Tris–HCl for 30 min at 22°C. Reactions were terminated by rapid filtration using a Brandell cell harvester. Radioactivity was measured using a Beckman LS5000TD liquid scintillation counter. Nonspecific binding was measured in the presence of 10 μM phentolamine.

[³H]prazosin competition curves Liver membranes (0.5 mg ml⁻¹ of protein) were incubated with 0.5 nM [³H]-prazosin in 50 mM Tris–HCl and a range of concentrations of competing ligands for 30 min at 22°C. The ligands used and the concentration ranges were as follows: prazosin: 1 pM–0.1 mM (nonselective), RS100329: 0.1 pM–10 μM (α_{1A}-AR selective) and BMY7378: 10 pM–1 mM (α_{1D}-AR selective). Nonspecific binding was measured in the presence of 10 μM phentolamine. Reactions were terminated and counted by the same method used for saturation assays.

Filter papers for all binding experiments were incubated with 0.3% polyethylenimine for 30 min before termination of reactions to reduce nonspecific binding.

Data analysis

Data are presented as mean ± s.e.m. Radioligand binding data were analysed using GraphPad Prism 3.01 (Institute for Scientific Information, CA, U.S.A.). Data from competition experiments were analysed using both one-site and two-site models. A two-site model was accepted only when the F ratio was found to be much greater than 1 and produced a P-value of less than 0.05. Hepatocyte images were analysed using Metamorph (Universal Imaging, U.S.A.) and then transferred into GraphPad Prism 3.01 for data manipulation. Statistical analysis was carried out using an unpaired t-test and a P-value of less than 0.05 was considered significant.

Solutions and drugs

The composition of the HEPES buffer used in all hepatocyte work was as follows (mM): NaCl (130), KCl (5), HEPES (20), glucose (10), $MgCl_2$ (1), $CaCl_2$ (1) – pH 7.4.

The composition of the Tris–HCl buffer used in all radioligand-binding experiments was as follows (mM): NaCl (150), Tris–HCl (50), EDTA (5), $MgCl_2$ (10) and 10% glycerol – pH 7.4.

The following compounds were used:

BMY7378 (dihydrochloride 8-[2-[4-(2-methoxyphenyl)-1-piperozynl]ethyl]-8-azaspiro(4,5)decone-7,9-dione, Research Biochemicals International, U.K.), Hepatocyte Attachment Media (Life Technologies), Hepatocyte Perfusion Media (Life Technologies), Hoescht 33342 (Molecular Probes, U.S.A.), phentolamine hydrochloride (Sigma, U.K.), polyethylenimine (Sigma, U.K.), [³H]prazosin hydrochloride (Amersham, U.S.A.), prazosin hydrochloride (Sigma, U.S.A.), QAPB (quinazolinyl piperazine-borate-dipyrromethene, marketed under the name BODIPY FL-prazosin, Molecular Probes, U.S.A.) and RS100329 (a gift from Dr Michelson, Roche Bioscience, U.S.A.).

Results

Fluorescence binding

Wild type QAPB displayed specific saturable binding to WT hepatocytes at both age points (Figure 1a), producing a characteristic pattern of fluorescence throughout the cell, with the exception of the nucleus. QAPB-associated fluorescence was abolished in the presence of 1 μM prazosin (Figure 1a). As the concentration of QAPB increased, the cellular distribution of fluorescence remained essentially similar, increasing in intensity until saturation was reached.

QAPB binding to individual hepatocytes occurred within the nanomolar range reported by other studies (Daly *et al.*, 1998; McGrath *et al.*, 1999; Mackenzie *et al.*, 2000; Sugawara *et al.*, 2002); however, the absolute amount of 'maximum' binding
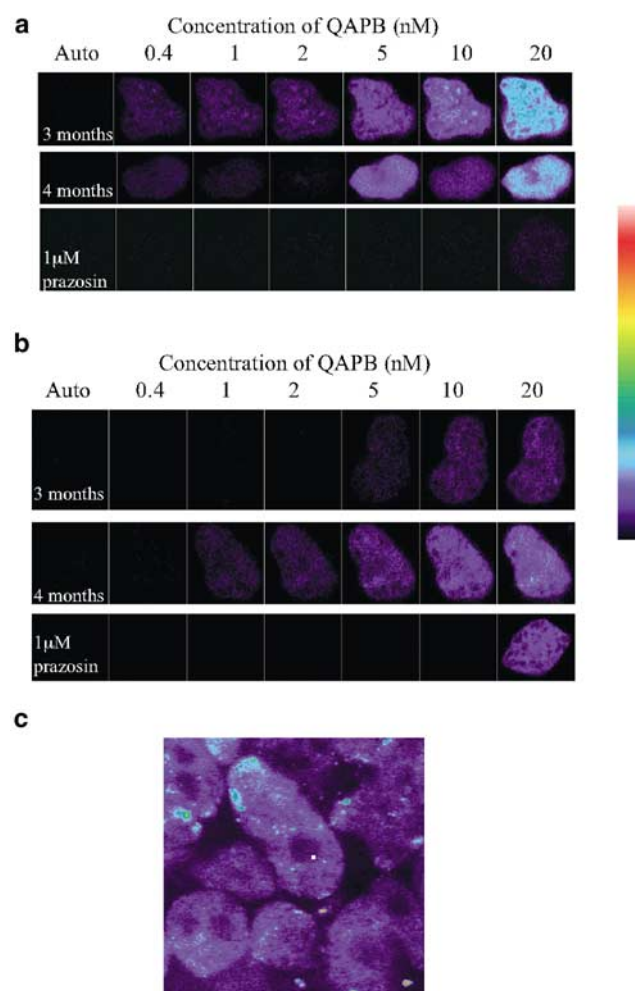
Figure 1 Typical QAPB binding on hepatocytes freshly isolated from livers of 3- and 4-month-old WT (a) and α_{1B}-AR KO (b) mice. Nonspecific binding was determined in the presence of 1 μM prazosin. Cells were plated on coverslips and examined by confocal microscopy with timelapse photography. Increasing concentrations (0.4–20 nM) were added cumulatively and images were collected at 1-min intervals. Images are presented in pseudocolour, where black indicates no staining, white indicates complete saturation and blue, cyan, yellow and red indicate increasing levels of saturation of the fluorophore, as indicated by pseudocolour scale. (c) 20 nM QAPB binding on WT liver slices. The image is a typical example of the results obtained ($n = 3$).

was quite heterogeneous; a proportion of cells did not bind QAPB specifically at all, whereas others could only produce a weak fluorescence and a third group of cells were found to produce a strong fluorescent signal. This made it impractical and misleading to calculate K_D and B_{max} values.

When QAPB binding was carried out on slices of WT liver, the distribution of α$_1$-ARs was similar to that found in isolated hepatocytes, that is, homogeneous distribution within cells but a heterogeneous distribution between groups of cells (Figure 1c).

α$_{1B}$-AR KO   The characteristics of QAPB-induced fluorescence were essentially similar in hepatocytes from the α$_{1B}$-AR KO mouse as in WT (Figure 1b). Binding was concentration-related, saturable and of high affinity. The pattern of fluorescence throughout the cell was similar to WT hepatocytes.

One difference, that was noticeable but difficult to quantify, was the evidence of low-affinity, high-intensity binding. This low-affinity binding was particularly noticeable at 3 months of age, probably as a consequence of fewer high-affinity binding sites.

These results make the completely novel and unexpected observation that, when the ontogenically expressed α$_{1B}$-AR is suppressed, a population of α$_1$-ARs is still present.

Competition binding   In WT hepatocytes, neither antagonists, RS100329 (α$_{1A}$-AR selective) or BMY7378 (α$_{1D}$-AR selective), were able to reduce the QAPB-associated fluorescence (Figure 2). In contrast to this, in α$_{1B}$-AR KO hepatocytes, the QAPB-associated fluorescence was completely abolished by RS100329, yet unaffected by BMY7378 (Figure 2).

These results reveal that WT hepatocytes express α$_{1B}$-ARs at 4 months of age, whereas α$_{1B}$-AR KO hepatocytes express α$_{1A}$-ARs.

A three-dimensional reconstruction of a single data set showing 5 nM QAPB binding on a WT mouse hepatocyte using the computer software IMARIS is shown in Figure 3. The image clearly shows the presence of α$_1$-ARs inside the cell, with no significant concentration of receptors associated with the plasma membrane.
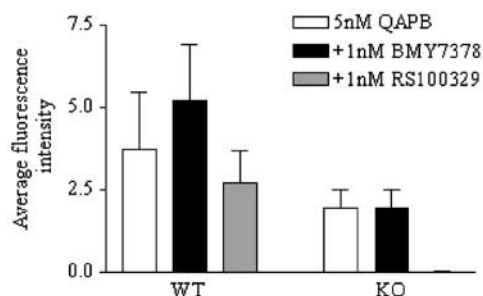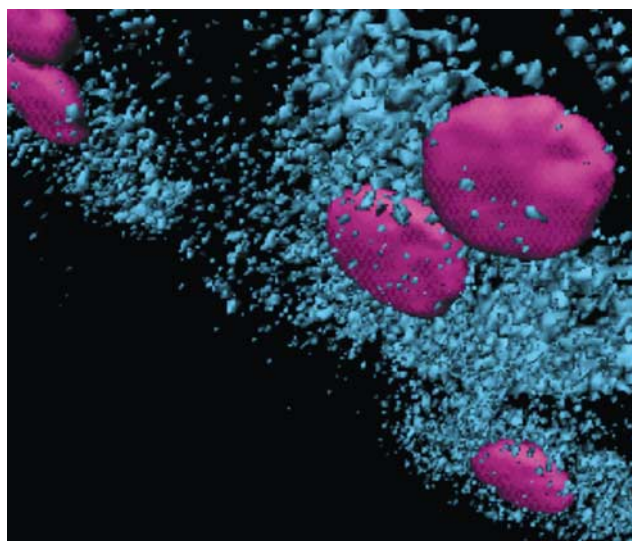

Figure 3   QAPB (5 nM) binding on a hepatocyte from freshly isolated WT mouse liver. Image was collected by confocal microscopy and the three-dimensional reconstruction performed by the computer software IMARIS. QAPB binding indicating the presence of α$_1$-ARs is shown in blue and propidium-iodide-staining-identifying nuclei are shown in pink.

Radioligand binding

Saturation binding   [^{3}H]prazosin demonstrated specific, saturable binding of high affinity at both ages in WT and α$_{1B}$-AR KO livers. K_D and B_{max} values are given in Table 1. The 3-month α$_{1B}$-AR KO livers had a significantly lower K_D value than their age-matched controls and the 4-month α$_{1B}$-AR KO. This could be a technical consequence of the lower expression level, but may also reflect a higher proportion of low-affinity sites, as shown in the fluorescence binding. Despite the significant differences, all K_D values were within the expected range for [^{3}H]prazosin (Bylund *et al.*, 1994).

The 3-month-old WT liver had a higher density of α$_1$-ARs than at 4 months of age, whereas the α$_{1B}$-AR KO had fewer α$_1$-ARs expressed at 3 months than at 4 months. These results show that the α$_1$-AR population in the α$_{1B}$-AR KO increases between 3 and 4 months of age, contrary to a slight decline in the WT population over this time period.

Competition binding   In WT liver, at both ages, all antagonists demonstrated competitive monophasic binding. Prazosin bound with nanomolar affinity consistent with binding to α$_1$-ARs (Bylund *et al.*, 1994), while RS100329 and BMY7378 bound with low affinities. pK_i values and Hill slopes are presented in Table 2.

In α$_{1B}$-AR KO livers, the density of α$_1$-ARs at 3 months was too low to allow accurate competitive binding to be carried out, so competition data for α$_{1B}$-AR KO livers was only obtained at 4 months. RS100329 and BMY7378 produced monophasic curves, competitive in nature. BMY7378 bound with low affinity, while RS100329 bound with high affinity, suggesting the presence of α$_{1A}$-ARs (Goetz *et al.*, 1995; Williams *et al.*, 1999). pK_i values and Hill slopes are presented in Table 3. These data confirm the results from fluorescent binding that WT liver expresses α$_{1B}$-ARs and α$_{1B}$-AR KO liver expresses α$_{1A}$-ARs. At this age, prazosin identified a minor

Figure 2   Bar chart representing 5 nM QAPB binding to 4-month-old WT and α$_{1B}$-AR KO hepatocytes pre-incubated with 1 nM BMY7378 or RS100329. Inhibition of QAPB binding was measured as the average fluorescence intensity of the cell compared to the average fluorescence intensity in the absence of inhibitor ($n \geqslant 3$).

Table 1 Comparison of [^{3}H]-prazosin binding to hepatic α_1-ARs from WT and α_{1B}-AR KO mice

	WT		*KO*	
	B_{max} (fmol mg^{-1})	K_D (nM)	B_{max} (fmol mg^{-1})	K_D (nM)
3 months	76±3.3	0.3±0.05	7.4±0.73[a]	1.0±0.27[a]
4 months	50±3.1[b]	0.3±0.08	30±2.0[a,b]	0.15±0.04[b]

B_{max} and K_D values obtained from saturation assays using [^{3}H]-prazosin in WT and α_{1B}-AR KO livers at 3 and 4 months of age ($n \geqslant 3$). $P < 0.05$.
[a]*versus* WT.
[b]*versus* 3 months.

Table 2 Comparison of affinity estimates at hepatic α_1 ARs for 3- and 4-month WT mice

	3 months		*4 months*	
	pK_i	$-n_H$	pK_i	$-n_H$
Prazosin	10.3±0.2	1.1±0.03	9.7±0.1	1.0±0.2
RS100329	7.3±0.03	0.98±0.06	7.8±0.02	1.0±0.04
BMY7378	6.2±0.04	1.17±0.08	6.3±0.02	1.0±0.05

Inhibition affinities in WT liver membranes expressed as pK_i values±s.e.m. Hill slopes (n_H) are expressed as the negative of the Hill slope±s.e.m. ($n \geqslant 3$).

Table 3 Comparison of affinity estimates at hepatic α_1 ARs for 4-month α_{1B} AR KO mice

	4 months	
	pK_i	$-n_H$
Prazosin	9.0±0.50, 7.0±0.23	0.50±0.1[a]
RS100329	9.3±0.07	0.82±0.1
BMY7378	6.2±0.09	0.9±0.15

Inhibition affinities in α_{1B}-AR KO liver membranes expressed as pK_i values±s.e.m. Hill slopes (n_H) are expressed as the negative of the Hill slope±s.e.m.
[a]Indicates a Hill slope which is significantly different from negative unity ($n \geqslant 3$).

(20%) low-affinity site in addition to the normal high-affinity site, similar to the biphasic response observed with fluorescent binding (Table 3).

Discussion

In this study, we have demonstrated that, when the normal population of α_{1B}-ARs is genetically suppressed, a new population of α_{1A}-ARs, with a similar cellular distribution, replaces them. To our knowledge, this is the first time that a direct substitution of a 'knocked out' AR has been demonstrated. In each of the three AR subfamilies, the 'response' of the mouse to deletion of a subtype has varied and is dependent on the tissue and function of the deleted receptor. There are examples where the KO of one subtype has revealed the presence of another that mediates a similar response (Devic *et al.*, 2001; Trendelenburg *et al.*, 2001; Daly *et al.*, 2002), but no compensatory upregulation has been reported. The phenomenon is unique so far to the liver and the α_1-AR family.

The time of appearance of the α_{1A}-AR in the α_{1B}-AR KO mouse between 3 and 4 months of age lags behind the onset of ontogenic expression of α_{1B}-AR. In the rat, the α_{1B}-AR replaces the foetal/neonatal β_2-AR that mediates adrenergic modulation of liver function in the first few weeks after birth (Rossby & Cornett, 1991). An earlier analysis by Cavalli *et al.* (1997) failed to detect α_1-ARs in livers of the α_{1B}-AR KO. Our demonstration of a sharp rise in α_{1A}-AR between 3 and 4 months suggests that the previous study used relatively young mice. From our own studies, it appears that the onset of expression of the α_{1A}-AR occurs just before 3 months of age since a small α_1-AR population was detected at 3 months, presumably α_{1A}-ARs.

The absence of α_{1A}-ARs in WT livers and its delayed onset in the α_{1B}-AR KO liver indicates that expression of the α_{1A}-AR in the α_{1B}-AR KO liver is a regulated compensation rather than an ontogenic age-dependent expression of α_{1A}-AR that is revealed when the α_{1B}-AR is suppressed. This shows that the α_{1A}-AR, although normally absent in WT mouse liver, is readily inducible, presumably in response to an error signal caused by the absence of a response normally met *via* the α_{1B}-AR. This offers an explanation for the 'species difference' in the functionally important α_1-AR subtype in the liver. Essentially any α_1-AR subtype could perform this biological role, since all act through the same G protein, $G_{q/11}$ and the same second messenger pathways. The factor(s) determining which α_1-AR subtype is expressed in a given species may depend on the environment or on other factors which influence metabolism.

Due to the unusual nature of the fluorescent binding, we carried out experiments using QAPB on liver slices. As with isolated cells, liver slices showed a homogeneous distribution within cells and a heterogeneous distribution between cells, validating our results from individual hepatocytes and confirming that this phenomenon is not a consequence of the dissociation procedure, but is in fact a characteristic of hepatocytes. The heterogeneous nature of the distribution of α_1-ARs throughout the liver has far-reaching consequences for adrenergic control of liver metabolism because it suggests that not all hepatocytes are under adrenergic control.

The distribution of α_1-ARs within isolated hepatocytes is novel, was unexpected and has interesting and far-reaching consequences. Some intracellular localization of any GPCR must be expected since receptors are synthesized inside the cell. The conventional view of GPCR function is that they mediate responses to extracellular signalling molecules that cannot penetrate the cell and that they activate, *via* G proteins, membrane-bound enzymes that produce second messengers that activate intracellular enzymes. In this scenario, intracellular receptors are either newly synthesized or engaged in a desensitization/resensitization recycling process. It may be that we have discovered that mouse hepatocyte α_1-ARs are located at intracellular sites awaiting mobilisation to the plasma membrane when required. If so, this is in itself interesting; however, we think that this is unlikely. Our evidence in mouse hepatocytes is so clearly against plasma membrane-bound receptors that we suggest a different view of hepatic α_1-ARs.

The concept of a plasma membrane location for ARs in hepatocytes would be inconsistent with their cell morphology. Hepatocytes consist of densely packed organelles, among which lie the glycogen storage granules. A second messenger produced at the plasma membrane would have a tortuous

journey to reach these. However, if the receptors were located in domains near to the targets, then signalling would be more efficient. The marshalling of receptors and subsequent elements in their signalling into discrete domains is of great current interest (Steinberg & Brunton, 2001; Zajchowski & Robbins, 2002). Such a scenario has been proposed for β_2-ARs in which essential components of their signalling cascade are localised to caveolae in myocyte membranes (Xiang *et al.*, 2002).

The distribution of ARs that we show here is not in line with the considerable literature on GPCRs and on hepatocytes. We believe that this is because we have applied an approach with high spatial resolution and high specificity for the receptor and have employed viable intact cells.

Our claim that there is no binding associated with the plasma membrane appears to be in conflict with radioligand-binding studies using liver membranes, including our own, which clearly detects binding associated with liver membranes. It seems likely, given the isolation procedures used by others and by us, that many types of membranes associated with the cell will have been isolated, for example, plasma membranes, mitochondrial membranes, lysosome membranes and endoplasmic reticulum. It is clear from our data, particularly the similar selectivity of antagonists against fluorescent and radioligand binding, that we are studying the same receptor populations with the two technologies.

This is not the first time that we have observed intracellular binding with QAPB in isolated cells, but what makes it unique in hepatocytes is that it is all inside. In human prostatic smooth muscle cells, 40% of QAPB binding was intracellular and was associated with the nucleus, though the greater part was distributed across the cell surface (Mackenzie *et al.*, 2000). A similar α_1-AR distribution was found in isolated vascular smooth muscle cells from rat basilar arteries (McGrath *et al.*, 1999). This makes sense in terms of an equilibrium involving receptor synthesis, plasma membrane localisation, desensitisation and recycling. The contrasting picture in the liver is quite unique.

In the 4-month-old α_{1B}-AR KO, the selective antagonists gave clear-cut inhibition of binding *versus* low concentrations of QAPB and [^{3}H]-prazosin, indicating a single population of 'α_{1A}-AR'. However, both the additional fluorescence found at high concentrations of QAPB and the minority 'low-affinity' site in the radioligand competition experiments with non-radioactive prazosin suggest a low-affinity site for these quinazolines. Low-affinity sites for prazosin are common in studies of α_{1A}-AR, and have been attributed to a phenomenon termed α_{1L}-AR, which is now considered to be an affinity state of the α_{1A}-AR (Ford *et al.*, 1997; Daniels *et al.*, 1999). High- and low-affinity sites for prazosin have been detected before in a binding study carried out by Ohmura & Muramatsu (1995) in rabbit liver. Using prazosin and other subtype-selective antagonists, they concluded that the rabbit liver expressed a mixed population of α_{1A}- and α_{1L}-ARs. However, going along with the hypothesis that the α_{1L}-AR is an affinity state of the α_{1A}-AR, it is possible that in the rabbit liver, where the α_{1A}-AR is expressed naturally, and the α_{1B}-AR KO mouse liver, where the α_{1A}-AR is upregulated, the high- and low-affinity states of the α_{1A}-AR can co-exist in the one tissue. To determine if this were the case would require further studies into the regulation of the α_{1A}-AR both in tissues in which it is naturally expressed and in tissues, such as the α_{1B}-AR KO mouse liver, where it has been upregulated.

In conclusion, we have shown for the first time that hepatic α_1-ARs are capable of compensating for one another in the absence of the endogenously expressed receptor. This compensation is age-dependent, highlighting the importance of age when using transgenic animals; compensatory mechanisms may be missed depending on the age point used. We also discovered that α_1-AR distribution in mouse liver is heterogeneous, being concentrated in a relatively small proportion of hepatocytes, and where it is expressed is distributed uniformly on intracellular organelles rather than on the cell surface. There was, however, no difference between the subcellular location and distribution of the 'normal' α_{1B}-ARs and the new α_{1A}-ARs that replaced them in the α_{1B}-AR KO liver. The ability of the α_{1B}-AR KO liver to express the α_{1A}-AR, the endogenously expressed human hepatic α_1-AR, may allow it to be exploited as a model of human hepatic AR mechanisms.

References

BYLUND, D.B., EIKENBERG, D.C., HIEBLE, J.P., LANGER, S.Z., LEFKOWITZ, R.J., MINNEMAN, K.P., MOLLINOF, P.B., RUFFOLO JR, R.R. & TRENDELENBURG, U. (1994). International Union of Pharmacology: nomenclature of ARs. *Pharmacol. Rev.*, **46**, 121–136.

CAVALLI, A., LATTION, A.-L., HUMMLER, E., NENNIGER, M., PEDRAZZINI, T., AUBERT, J.-F., MICHEL, M.C., YANG, M., LEMBO, G., VECCHIONE, C., MOSTARDININ, M., SCMIDT, A., BEERMANN, F. & COTECCHIA, S. (1997). Decreased blood pressure response in mice deficient of the α_{1b}-AR. *Proc. Natl. Acad. Sci. U.S.A.*, **94**, 11589–11594.

CHALATHORN, D., MCCUNE, D.F., EDELMANN, S.E., GARCIA-CAZARIN, L., TSUJIMOTO, G. & PIASCIK, M.T. (2002). Differences in the cellular localisation and agonist-mediated internalisation properties of the α_1-AR subtypes. *Mol. Pharmacol.*, **61**, 1008–1116.

DALY, C.J., DEIGHAN, C., MCGEE, A., MENNIE, D., ALI, Z., MCBRIDE, M. & MCGRATH, J.C. (2002). A knockout approach indicates a minor vasoconstrictor role for vascular α_{1B}-ARs in mouse. *Physiol. Genomics*, **9**, 85–91.

DALY, C.J., MILLIGAN, C.M., MILLIGAN, G., MACKENZIE, J.F. & MCGRATH, J.C. (1998). Cellular localization and pharmacological characterization of functioning α_1-ARs by fluorescent ligand binding and image analysis reveals identical binding properties of clustered and diffuse populations of receptors. *J. Pharmacol. Exp. Ther.*, **286**, 984–990.

DANIELS, V.D., GEVER, J.R., JASPER, J.R., KAVA, S., LESNICK, J.D., MELOY, T.D., STEPAN, G., WILLIAMS, T.J., CLARKE, D.E., CHANG, D.J. & FORD, A.P.D.W. (1999). Human cloned α_{1A}-AR isoforms display α_{1L}-AR pharmacology in functional studies. *Eur. J. Pharmacol.*, **370**, 337–343.

DAVID, P., VIOLLON, C., ALEXANDRE, E., AZIMZADEH, A., NICOD, L., WOLF, P., JAECK, D., BOUDJEMA, K. & RICHERT, L. (1998). Metabolic capacities in cultured human hepatocytes obtained by a new isolating procedure from non-wedge small liver biopsies. *Hum. Exp. Toxicol.*, **17**, 544–553.

DEIGHAN, C. & MCGRATH, J.C. (2002). The expression levels of hepatic α1-ARs change with age in α_{1B}-AR KO mice. *Br. J. Pharmacol.,* **137,** 20.

DEIGHAN, C., SLATTERY, D.A., MACKENZIE, J.F., COTECCHIA, S. & MCGRATH, J.C. (1999). The characterisation of α_1-ARs in murine liver using radioligand binding and transgenic mice. *Br. J. Pharmacol.,* **128,** 91.

DEVIC, E., XIANG, Y., GOULD, D. & KOBILKA, B. (2001). β-AR subtype-specific signaling in cardiac myocytes from β_1- and β_2-AR knockout mice. *Mol. Pharmacol.,* **60,** 577–583.

FORD, A.P.D.W., DANIELS, D.V., CHANG, D.J., GEVER, J.R., JASPER, J.R., LESNICK, J.D. & CLARKE, D.E. (1997). Pharmacological pleiotropism of the human recombinant α_{1A}-AR: implications for α_1-AR classification. *Br. J. Pharmacol.,* **121,** 1127–1135.

GARCIA-SAINZ, J.A., CASAS-GONZALEZ, P., ROMERO-AVILA, M.T. & GONZALEZ-ESPINOSA, C. (1994). Characterization of the hepatic α_{1B}-ARs of rats, mice and hamsters. *Life Sci.,* **52,** 1995–2003.

GARCIA-SAINZ, J.A., GARCIA-CABALLERO, A. & GONZALEZ-ESPINOSA, C. (1996a). Characterization of the α_1-ARs of cat liver. Predominance of the α_{1A}-adrenergic subtype. *Life Sci.,* **59,** 235–242.

GARCIA-SAINZ, J.A., ROMERA-AVILA, M.T., ALCANTARA-HERNANDEZ, R., MACIAS-SILVA, M., OLIVARES-REYES, A. & GONZALEZ-ESPINOSA, C. (1992). Species heterogeneity of hepatic α_1-ARs: α_{1A}-, α_{1B}- and α_{1C}-subtypes. *Biochem. Biophys. Res. Commun.,* **186,** 760–767.

GARCIA-SAINZ, J.A., ROMERO-AVILA, M.T. & GONZALEZ-ESPINOSA, C. (1995a). Characterization of the α_1-ARs of the dog liver: predominance of the α_{1A}-subtype. *Eur. J. Pharmacol.,* **272,** 139–143.

GARCIA-SAINZ, J.A., ROMERO-AVILA, M.T. & GONZALEZ-ESPINOSA, C. (1996b). Coexpression of α_{1A}- and α_{1B}-ARs in the liver of the rhesus monkey (*Macaca mulatta*). *Eur. J. Pharmacol.,* **311,** 277–283.

GARCIA-SAINZ, J.A., ROMERO-AVILA, M.T. & TORRES-MARQUEZ, E. (1995b). Characterization of the human liver α_1-ARs: predominance of the α_{1A} subtype. *Eur. J. Pharmacol.,* **289,** 81–86.

GOETZ, A.S., KING, H.K., WARD, S.D.C., TRUE, T.A., RIMELE, T.J. & SAUSSY, D.L. (1995). BMY7378 is a selective antagonist of the D subtype of α_1-ARs. *Eur. J. Pharmacol.,* **272,** R5–R6.

HAGUE, C., UBERTI, M.A., CHEN, Z., HALL, R.A. & MINNEMAN, K.P. (2004). Cell surface expression of α_{1D}-ARs is controlled by heterodimerisation with α_{1B}-ARs. *J. Biol. Chem.,* **279,** 15541–15549.

HIEBLE, J.P., BYLUND, D.B., CLARKE, D.E., EIKENBERG, D.C., LANGER, S.Z., LEFKOWITZ, R.J. & MINNEMAN, K.P. (1995). International Union of Pharmacology X. Recommendation for nomenclature of α_1-ARs: consensus update. *Pharmacol. Rev.,* **47,** 267–270.

HROMETZ, S.L., EDELMANN, S.E., MCCUNE, D.F., OLGES, J.R., HADLEY, R.W., PEREZ, D.M. & PIASCIK, M.T. (1999). Expression of multiple α_1-ARs on vascular smooth muscle: correlation with the regulation of contraction. *J. Pharmacol. Exp. Ther.,* **290,** 452–463.

MACKENZIE, J.F., DALY, C.J., PEDIANI, J.D. & MCGRATH, J.C. (2000). Quantitative imaging in live human cells reveals intracellular α_1-AR ligand-binding sites. *J. Pharmacol. Exp. Ther.,* **294,** 434–443.

MCGRATH, J.C., MACKENZIE, J.F. & DALY, C.J. (1999). Pharmacological implications of cellular localisation of α_1-ARs in native smooth muscle cells. *J. Auton. Pharmacol.,* **19,** 303–310.

OHMURA, M. & MURAMATSU, I. (1995). Two distinct α_1-AR subtypes in rabbit liver: a binding study. *Br. J. Pharmacol.,* **116,** 2591–2596.

ROSSBY, S. & CORNETT, L.E. (1991). Steady state levels of hepatic α_1- and α_2-ARs and gene transcripts during development of the male rat. *J. Cell. Physiol.,* **145,** 55–61.

STANASILA, L., PEREZ, J.B., VOGEL, H. & COTECCHIA, S. (2003). Oligomerization of the α_{1a}- and α_{1b}-AR subtypes. Potential implications in receptor internalization. *J. Biol. Chem.,* **278,** 40239–40251.

STEINBERG, S.F. & BRUNTON, L.L. (2001). Compartmentation of G protein-coupled signalling pathways in cardiac myocytes. *Annu. Rev. Pharmacol. Toxicol.,* **41,** 751–753.

SUGAWARA, T., HIRASAWA, A., HASHIMOTO, K. & TSUJIMOTO, G. (2002). Differences in the subcellular localisation of α_1-AR subtypes can affect the subtype selectivity of drugs in a study with the fluorescent ligand BODIPY FL-prazosin. *Life Sci.,* **70,** 2113–2124.

TRENDELENBURG, A.U., NORENBERG, W., HEIN, L., MEYER, A. & STARKE, K. (2001). α_2-AR mediated inhibition of cultured sympathetic neurons: changes in $\alpha_{2A/D}$-AR deficient mice. *Naunyn-Schmiedeberg's Arch. Pharmacol.,* **363,** 110–119.

TSUJIMOTO, G., HIRASAWA, A., SUGAWARA, T. & AWAJI, T. (1998). Subtype-specific differences in subcellular localisation and chloroethylclonidine inactivation of α_1-ARs. *Life Sci.,* **62,** 1567–1571.

WILLIAMS, T.J., BLUE, D.R., DANIELS, D.V., DAVIS, B., ELWIRTHY, T., GEVER, J.R., KAVA, M.S., MORGANS, D., PADILLA, F., TASSA, S., VIMONT, R.L., CHAPPLE, C.R., CHESS-WILLIAMS, R., EGLEN, R.M., CLARKE, D.E. & FORD, A.P.D.W. (1999). *In vitro* α_1-AR pharmacology of Ro 70-0004 and RS-100329, novel α_{1A}-AR selective antagonists. *Br. J. Pharmacol.,* **127,** 252–258.

XIANG, Y., RYBIN, V.O., STEINBERG, S.F. & KOBILKA, B. (2002). Caveolar localisation dictates physiologic signalling of β_2-ARs in neonatal cardiac myocytes. *J. Biol. Chem.,* **277,** 34280–34286.

YANG, M., REESE, J., COTECCHIA, S. & MICHEL, M.C. (1998). Murine α_1-AR subtypes. I. Radioligand binding studies. *J. Pharmacol. Exp. Ther.,* **286,** 841–847.

ZAJCHOWSKI, L.D. & ROBBINS, S.M. (2002). Lipid rafts and little caves. Compartmentalised signalling in membrane microdomains. *Eur. J. Biochem.,* **269,** 737–752.